

706  
707  
708  
709  
710  
711  
712  
713  
714  
715  
716  
717  
718  
719  
720  
721  
722  
723

724 **Supplementary Fig. 1, related to Fig. 1. Alphafold2 prediction of IER5 structure and**  
725 **PP2A/B55 $\alpha$ -IER5 purification for cryo-EM structure determination. A and B, Alphafold2<sup>31</sup>**  
726 prediction of the IER5 structure, shown in cartoon representation. A, pLDDT coloring of IER5  
727 using alphafold palette: <50, red, very low confidence; 50-70, yellow, low confidence; 70-90,  
728 light blue, confident; 90-100, dark blue, very high confidence. B, Cartoon representation of  
729 IER5 with the IER-N50 domain colored cyan. The 1-50 region is also highlighted in cyan on  
730 the domain representation beneath the cartoon. C, Size exclusion chromatogram of the  
731 purified PP2A/B55 $\alpha$ -IER5 complex on a Superdex 200 column. An SDS-PAGE gel of the

732 purified complex is shown to the right of the chromatogram. Both peaks are PP2A/B55 $\alpha$ -IER5  
733 complexes; peak 2 was used in all biochemical and structural studies.

734

735 **Supplementary Fig. 2, related to Fig. 1. Cryo-EM image processing workflow.** Cryo-EM  
736 processing scheme for PP2A/B55 $\alpha$ -IER5 reconstruction. Milestone maps are shown to display  
737 progression of processing (the discarded, “junk” class is shown as pink, the monomer as  
738 orange, the dimer as blue, and the combined map as purple). The masks used for local  
739 refinement are light blue.

740

741 **Supplementary Fig. 3, related to Fig. 1. Cryo-EM data quality.** A, Representative  
742 micrograph of PP2A-IER5 in vitreous ice visualized by cryo-EM on a Titan Krios microscope  
743 equipped with a Gatan K3 detector. Scale bar indicates 500 Å. B, GS-FSC curves with default  
744 CryoSPARC masks. C, Orientation distribution of particles (from CryoSPARC) used in  
745 preparing the final map of PP2A/B55 $\alpha$ -IER5 for model building. D, 2D class averages of  
746 PP2A/B55 $\alpha$ -IER5 reconstruction prior to particle subtraction. E, Local resolution map of the  
747 final map generated by CryoSPARC (FSC threshold = 0.143). F, map-model FSC curve (line  
748 at FSC = 0.5) generated using Phenix<sup>55</sup>. G, Maps around IER5 helix 1 (left), loop (loop) and  
749 helix 2 (right). Sigma was set to 3. All maps shown were processed using DeepEMhancer<sup>46</sup>.

750

751 **Supplementary Fig. 4, related to Figs. 1 and 2. Comparison of the PP2A/B55 $\alpha$  - IER5**  
752 **complex with PP2A/B55 $\alpha$  structures bound to other partners.** A, superposition of  
753 PP2A/B55 $\alpha$  bound to microcystin-LR<sup>9</sup> (MC-L complex, protein subunits in gray, microcystin-  
754 LR as salmon sticks) on the structure of the PP2A/B55 $\alpha$  complex with IER5. In the IER5  
755 complex, the B55 $\alpha$  subunit is purple, the catalytic subunit is wheat, the scaffolding subunit is  
756 green, and IER5 is cyan. Helices are depicted as solid cylinders. Alignment was performed on  
757 the B55 $\alpha$  subunit. Note the increased curvature of the scaffolding subunit and the 22 Å

758 displacement of its C terminus in the IER5 structure relative to the microcystin-LR structure.  
759 B, Comparison showing the different binding modes of IER5, ARPP19 and FAM122A when  
760 bound to PP2A/B55 $\alpha$ <sup>11</sup>. Structures are shown in cartoon representation with a transparent  
761 surface. The three PP2A subunits are colored as in (A), with IER5 in cyan, ARPP19 in blue,  
762 and FAM122A in red. Structures were aligned on the B55 $\alpha$  subunit. C, Surface representations  
763 of B55 $\alpha$  (purple) with bound IER5-N50 (cyan) shown in cartoon representation. On each copy,  
764 surface residues of B55 $\alpha$  important for IER5-N50 binding or substrate recruitment are painted  
765 a different color from left to right: IER5-N50, pink surface; p107<sup>25</sup>, blue surface; PRC1<sup>26</sup>, yellow  
766 surface; pTau<sup>9</sup>, green surface.

767

768 **Supplementary Fig. 5, related to Figs. 1 and 2.** A, Size exclusion chromatogram of the  
769 purified PP2A/B55 $\alpha$  complex on a Superdex 200 column. An SDS-PAGE gel of the purified  
770 complex is shown to the right of the chromatogram. The peak at approximately 20 mL elution  
771 volume corresponds to the FLAG peptide. B, SDS-PAGE gels of purified MBP-fusions for  
772 IER5-N50, IER5-N50 K17E, IER5-FL and IER5-FL K17E.

773

774

775

776 **Table S1, related to Fig. 5. Predictions of complex structures between IER/SERTAD**  
777 **superfamily proteins and PP2A/B55 $\alpha$ .** Structures of complexes between IER, SERTAD, and

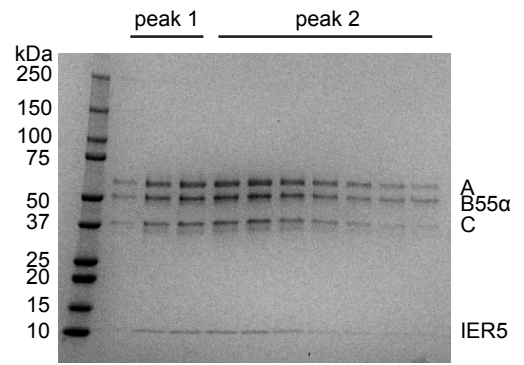
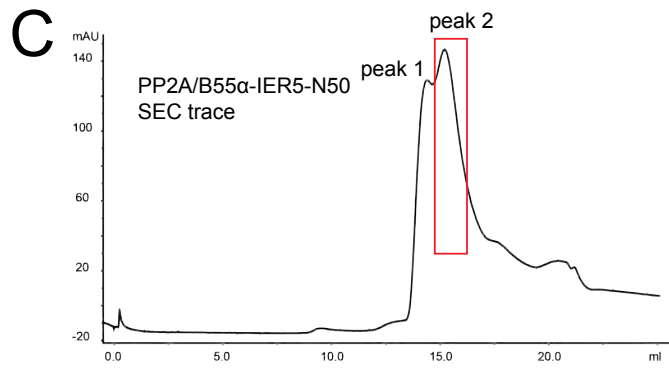
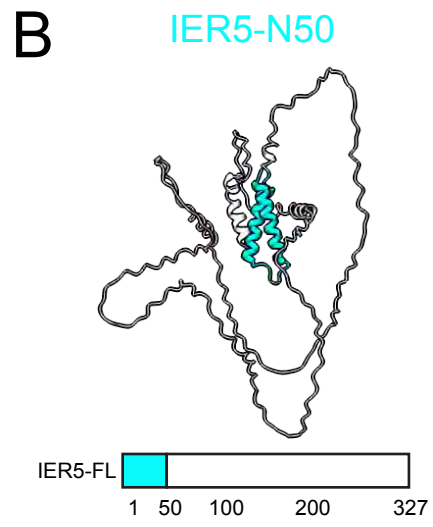
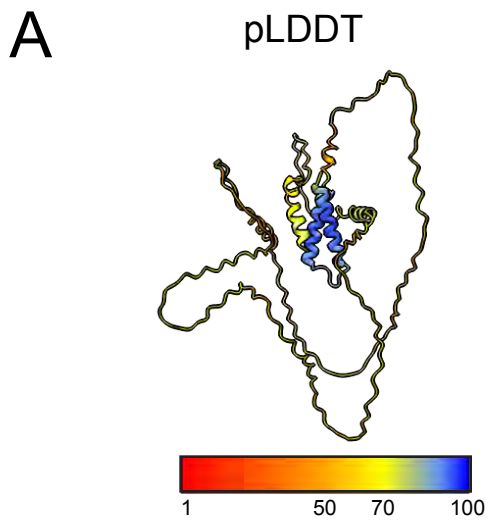


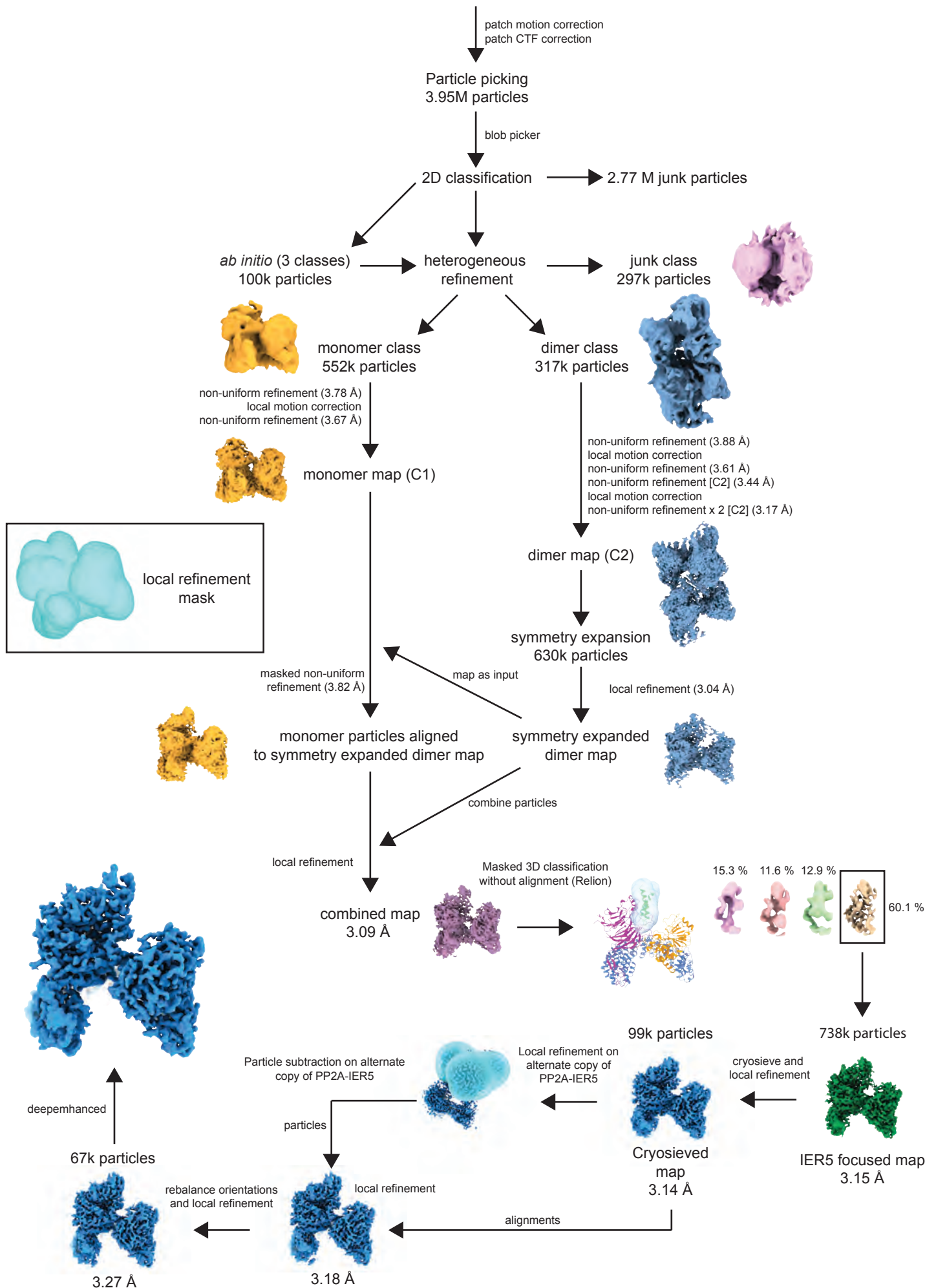
778 CDCA4 proteins with PP2A/B55 $\alpha$  heterotrimers were predicted using alphafold2<sup>31</sup> (Fig. 5) and  
779 scored using predictomes<sup>56</sup>. Each column shows a metric used to score the predictive value  
780 of the model. Average models indicate the mean number of interface contacts observed for  
781 the five models that were generated. The maximum (max) number of models counts how many  
782 models share one or more of the predicted contacts in other models. Predicted Dockq  
783 (pDOCKq) is a metric that incorporates the alphafold2 pLDDT scores across the predicted  
784 protein-protein interaction interface<sup>57</sup>. Predicted local distance difference test (pLDDT), and  
785 predicted alignment error (PAE) are alphafold2 metrics<sup>31</sup>.

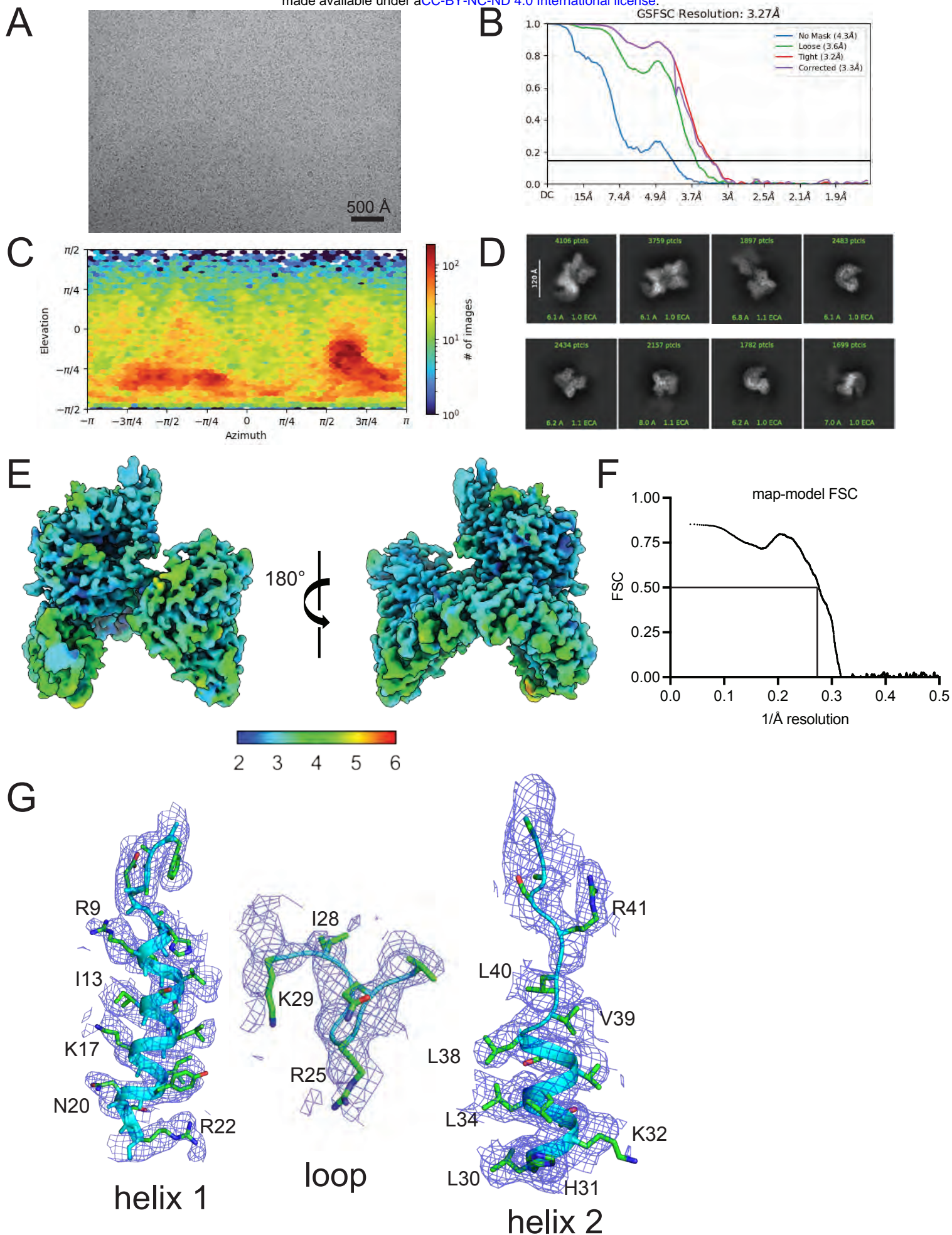
Protein	average models	max number of models	best model	best model pDockQ	best model pLDDT	best model PAE
SRTD4	4.8	5	4	0.713	87.7	1.8
SRTD2	4.7	5	4	0.72	90	1.6
STD1	4.7	5	4	0.722	91.5	1.4
CDCA4	4.6	5	4	0.715	89.9	1.6
IER5	4.5	5	4	0.714	88.1	1.6
IER5L	4.4	5	4	0.714	88.5	1.4
IER2	4.4	5	4	0.713	87.7	1.7
SRTD3	4.4	5	3	0.714	88.1	1.7

786

787

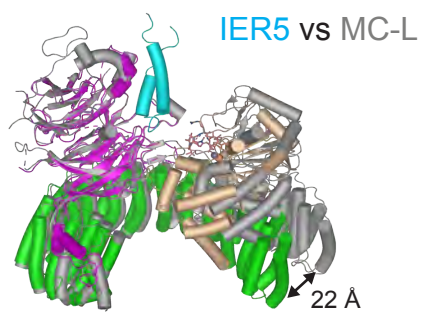




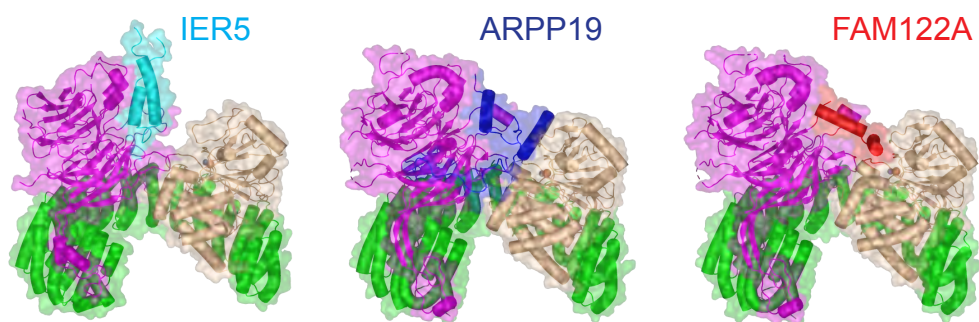




A



B



C

